REGULAR ARTICLE

blood advances

Pharmacological DNA demethylation restores SMAD1 expression and tumor suppressive signaling in diffuse large B-cell lymphoma

Anna Stelling,[1] Cheuk-Ting Wu,[1] Katrin Bertram,[1] Hind Hashwah,[1] Alexandre P. A. Theocharides,[2,3] Markus G. Manz,[2,3] Alexandar Tzankov,[4] and Anne Müller[1,3]

[1]Institute of Molecular Cancer Research, Zurich, Switzerland; [2]Department of Medical Oncology and Hematology, University Hospital Zurich and University of Zurich, Zurich, Switzerland; [3]Comprehensive Cancer Center Zurich, Zurich, Switzerland; and [4]Institute of Pathology, University Hospital Basel, Basel, Switzerland

Key Points

- SMAD1 is silenced by hypermethylation in DLBCL cell lines and patient samples but not in peripheral blood B cells or lymph nodes.
- DAC treatment restores SMAD1 expression and reverses DLBCL growth in several xenotransplantation and patient-derived xenograft models.

The sphingosine-1-phosphate (S1P) receptor S1PR2 and its downstream adaptor Gα13 are recurrently mutationally inactivated in the germinal center B-cell subtype of diffuse large B-cell lymphoma (DLBCL) and are silenced by the S1PR2 repressor FOXP1 in the activated B-cell like subtype of the disease. Loss of S1PR2 signaling relieves the germinal center confinement that is maintained by an S1P gradient and allows cells to resist S1P-induced apoptosis. We have shown previously that S1PR2 expression is induced in normal B cells through a newly described transforming growth factor-β (TGF-β)/TGF-βRII/SMAD1 signaling axis that is inactivated in >85% of DLBCL patients. DLBCL cell lines lacking *S1PR2*, *TGFBRII*, or *SMAD1* as the result of genomic editing all have a strong growth advantage in vitro, as well as in subcutaneous and orthotopic xenotransplantation models. Here, we show that the TGF-β signaling pathway in DLBCL is blocked at the level of SMAD1 in DLBCL cell lines and patient samples by hypermethylation of CpG-rich regions surrounding the *SMAD1* transcription start site. The pharmacologic restoration of SMAD1 expression by the demethylating agent decitabine (DAC) sensitizes cells to TGF-β–induced apoptosis and reverses the growth of initially SMAD1$^-$ cell lines in ectopic and orthotopic models. This effect of DAC is reduced in a SMAD1-knockout cell line. We further show that DAC restores SMAD1 expression and reduces the tumor burden in a novel patient-derived orthotopic xenograft model. The combined data lend further support to the concept of an altered epigenome as a major driver of DLBCL pathogenesis.

Introduction

Diffuse large B-cell lymphoma (DLBCL) is the most common lymphoid malignancy in adults and is characterized by substantial clinical and genetic heterogeneity. Comprehensive genetic analyses that considered copy number variations, structural aberrations, point mutations and other genetic abnormalities, transcriptional profiles, and clinical data from hundreds of patients have allowed the stratification of DLBCL into 4 or 5 subtypes that differ in their cell of origin and associated transcriptional signatures, mutational signatures, and clinical prognosis.[1,2] These multiomics approaches have revealed that classification into activated B-cell (ABC) and germinal center B-cell (GCB)–like subtypes of DLBCL based on transcriptional signatures and cell of origin,[3,4] which was the gold standard for >15 years, fails to capture the clinical heterogeneity of the disease. In particular, the stratification of patients based on co-occurring mutations has uncovered a previously unappreciated favorable-risk ABC DLBCL subtype with genetic features of an extrafollicular, and possibly marginal zone, origin and has divided GCB DLBCL into poor-risk (with structural aberrations in *BCL2* and alterations of *PTEN* and epigenetic enzymes) and good-risk categories, with distinct alterations in *BCR/PI3K*, *JAK/STAT*, and *BRAF*.[1]

Submitted 27 March 2019; accepted 20 August 2019. DOI 10.1182/bloodadvances.2019000210.

For original data, please contact Anne Müller (mueller@imcr.uzh.ch).

The full-text version of this article contains a data supplement.

© 2019 by The American Society of Hematology

Despite these recent advances, very few genetic abnormalities are likely to be exploited clinically in the near future. Among these are inhibitors that interfere with chronic active B-cell receptor signaling at the level of Bruton's tyrosine kinase, which are projected to show efficacy primarily in ABC DLBCL patients with co-occurring *CD79* and *MYD88* mutations[2,5] and aberrations affecting Bcl-2 expression, which could potentially be targeted by BH3 mimetics, such as venetoclax.[6] In addition to the genetic diversity that is a hallmark of DLBCL, aberrations of the epigenome are increasingly recognized as a major driver of DLBCL pathogenesis. DLBCL cell lines and primary samples differ substantially in terms of their global DNA methylation and CpG island–specific DNA methylation profiles.[7,8] Mutations in epigenetic modifiers are among the most commonly occurring in both subtypes of DLBCL,[9-11] and mutations in histone acetyltransferase–encoding genes have been associated with especially poor outcomes.[12,13] Because the repressive histone marks that are affected by loss- or gain-of-function mutations in histone methyltransferases (HMTs) and histone acetyltransferases (*KMT2D*, *EZH2*, *CREBBP*, *EP300*) are directly linked to aberrant DNA methylation,[14-16] it is likely that the dysregulation of histone modifications driven by some of these mutations affects (tumor suppressor) gene expression.

We and other investigators have identified the G protein–coupled receptor sphingosine-1-phosphate (S1P) receptor 2 (S1PR2) to be recurrently inactivated or silenced in both cell-of-origin–derived DLBCL subtypes. In GCB DLBCL, the genes encoding S1PR2 and its downstream adaptor Gα13 (*GNA13*) are recurrently inactivated by point mutations.[17] In ABC DLBCL, the expression of S1PR2 is silenced as a consequence of overexpression of its transcriptional repressor FOXP1.[18] Irrespective of subtype, the loss of S1PR2 signaling provides a major growth advantage to DLBCL cells in vitro and in vivo: introducing the *S1PR2*-inactivating mutation by CRISPR-mediated genome editing generates clones that grow faster in vitro and that engraft and form ectopic and orthotopic lymphomas more rapidly than the parental wild-type (WT) cell line.[19] Conversely, the inducible expression of WT S1PR2, but not of a point mutant incapable of activating downstream signaling pathways, induces apoptosis in DLBCL cells and restricts tumor growth in subcutaneous and orthotopic models of the disease.[18] In a genetically engineered mouse model of MYC-driven lymphoma, the loss of *S1pr2* accelerates spontaneous lymphomagenesis and confers a growth advantage to serially transplanted lymphoma cells.[18,19] We reported recently that S1PR2 is negatively regulated by FOXP1 and that the same regulatory elements of the *S1PR2* gene are also bound by an activating transcription factor, SMAD1.[19] Thus, optimal expression of S1PR2 occurs only if FOXP1 is absent and SMAD1 is expressed, activated, and has translocated into the nucleus. SMAD1 activation through its tyrosine phosphorylation occurs as a consequence of transforming growth factor-β (TGF-β) signaling. Indeed, the genetic deletion of *SMAD1* or *TGFBRII* phenocopies the effects of *S1PR2* loss in vitro and in vivo in various genetically modified and xenotransplantation models.[19] We have shown by immunohistochemical analysis of SMAD1 expression in 2 large DLBCL patient cohorts that the TGF-β/TGF-βRII/SMAD1 axis is dysregulated at the level of SMAD1 expression, which is aberrantly low in >85% of DLBCL patients.[19] Here, we have examined the mechanistic basis of SMAD1 silencing in DLBCL cell lines and patient biopsies and show that the hypermethylation of 5 regions surrounding the *SMAD1* transcription start site likely accounts for the lack of SMAD1 expression that we observed in the majority of cell lines and patient samples that were examined in this study. The restoration of SMAD1 expression by the demethylating agent decitabine (DAC) rescues S1PR2 expression, as well as sensitizes cells to TGF-β–induced apoptosis and reduces the ectopic and orthotopic growth of DLBCL cell lines and primary cells in vitro and in vivo.

Methods

Cell culture

The DLBCL cell lines used included 6 of the GCB DLBCL subtype (SU-DHL-4, SU-DHL-5, SU-DHL-6, SU-DHL-8, SU-DHL-10, SU-DHL-16), 4 of the ABC DLBCL subtype (U2932, OCI-Ly3, SU-DHL-2, and RIVA), and 1 unclassified cell line (RC-K8). Selected cell lines were subjected to various concentrations of DAC (Sigma-Aldrich) or human TGF-β1 (referred to as TGF-β) (PeproTech). DAC-treated cells were analyzed with respect to *SMAD1* and *S1PR2* expression by quantitative reverse-transcription polymerase chain reaction (qRT-PCR), apoptosis by annexin V staining, and SMAD1 protein expression by western blot. Cell lines were labeled with luciferase via lentiviral transfer and subjected to *SMAD1* deletion via CRISPR/Cas9 manipulation; they were also subjected to bisulfite sequencing of the *SMAD1* promoter region. Culture conditions, treatment conditions, apoptosis assays, RNA extraction and qRT-PCR, western blotting technique, lentiviral gene transfer, *SMAD1* CRISPR manipulations, and bisulfite sequencing are described in supplemental Material and methods.

Animal experimentation

NOD/SCID/IL2Rγ$^{-/-}$ (NSG) mice, CSF^{h};IL-3/GM-CSF^{h};hSIRPA^{tg};TPO^{h};Rag2^{-};γc^{-} (MISTRG) mice, and CSF^{h};IL-3/GM-CSF^{h};hSIRPA^{tg};TPO^{h};Rag2^{-};γc^{-};IL6^{h} (MISTRG6) mice[11] were obtained from a local repository. For xenotransplantation studies, RC-K8 or SU-DHL-4 cells (20×10^6 or 10×10^6 cells, respectively, in 200 μL of phosphate-buffered saline [PBS]) were injected subcutaneously into both flanks of 6- to 8-week-old NSG mice. Once palpable tumors had formed in the subcutaneous model, the volume of the tumors was measured by calipers and calculated using the formula $(A^2 \times B)/2$, where A is the shorter tumor dimension and B is the longer tumor dimension. From day 12, mice were injected intraperitoneally with 0.25 or 0.5 mg/kg 5-aza-2′-deoxycytidine (referred to as DAC, reconstituted in PBS; Sigma-Aldrich) or PBS as control for 5 consecutive days per week for 2 weeks. For orthotopic in vivo imaging system (IVIS) studies, 10×10^6 luciferase-labeled RC-K8, SU-DHL-6, or SU-DHL-4 cells were injected IV in a volume of 100 μL into 6- to 8-week-old MISTRG or MISTRG6 mice[11] to evaluate orthotopic growth. Mice were imaged once a week to determine the dissemination of cells. For DAC treatment studies, after 2 to 3 weeks, when engrafted cells could be detected in all experimental animals, mice were injected intraperitoneally with 0.25 mg/kg DAC or PBS as control for 5 consecutive days per week for 3 weeks. For the patient-derived xenograft transplantation model, bone marrow mononuclear cells containing DLBCL cells (obtained from the Clinic of Hematology-Oncology, University of Zurich) from a consenting patient with stage IVBE ABC DLBCL with extranodal manifestations in the liver and ~7% tumor cell infiltration of the marrow, who was selected because of aberrantly high *SMAD1* methylation in the tumor cells, were injected IV into MISTRG6 mice. A total of 1.5×10^6 lymphoma

cells that had engrafted in the spleen was serially transplanted into MISTRG6 mice, and mice were treated 2 weeks after injection with 0.25 mg/kg DAC or PBS as control for 5 consecutive days per week for 3 weeks. At the end point, spleen and bone marrow cells were subjected to fluorescence-activated cell sorting (FACS) analysis of $CD45^+$ cells. FACS analysis is described in supplemental Material and methods. All animal studies were reviewed and approved by the Zurich Cantonal Veterinary Office (licenses 227/2015, 235/2015). Ethical approval for work with primary DLBCL cells was obtained from the Ethical Commission of the Canton of Zurich (KEK-ZH No. 2009-0062/1).

SMAD1 immunohistochemistry on patient samples and SMAD1 immunofluorescence microscopy of cell lines

Expression of SMAD1 was studied by immunohistochemistry on 6 DLBCL patient samples (3 nodal, 1 lung, and 2 testicular). Of the 3 nodal samples, 1 was classified as GCB and 2 were classified as non-GCB, according to the Hans classification that takes CD10, BCL-6, and MUM1 expression into account and is ~80% accurate in stratifying DLBCL into GCB and non-GCB subsets.[20] The 2 testis DLBCL samples were classified as non-GCB, with 1 exhibiting a BCL-6 rearrangement and the other exhibiting *KMT2D* and *PIM1* mutations. The lung DLBCL case was also non-GCB. The primary polyclonal antibody (cs9743; Cell Signaling Technology) was diluted 1:40 and incubated for 20 minutes in an automated immunostainer (BenchMark; VENTANA/Roche) after heat-induced antigen retrieval with CC1 buffer for 40 minutes. DNA was extracted from the same samples and subjected to bisulfite sequencing. Bisulfite sequencing is described in supplemental Material and methods. For SMAD1 immunofluorescence microscopy, cells were fixed for 15 minutes in 4% paraformaldehyde, permeabilized for 5 minutes in 1% NP-40, and stained for 90 minutes in the same primary antibody (1:40 dilution; cs9743; Cell Signaling Technology) as used for immunohistochemistry, followed by labeling with goat anti-rabbit secondary antibody (Life Technologies; 1:200 dilution) for 60 minutes. Images were acquired with a Leica DM6B fluorescence microscope.

Statistics

All statistical analyses were performed using GraphPad Prism software. Graphs represent mean plus standard error of the mean (SEM) for ≥3 independent experiments for cell culture experiments and medians for mouse experiments, unless indicated otherwise in the figure legend. Statistical analysis was performed using a 2-tailed Student *t* test for in vitro assays and a 2-tailed Mann-Whitney *U* test for in vivo studies.

Results

SMAD1 is silenced by DNA methylation of its promoter region in the majority of DLBCL cell lines and primary human DLBCL

Having reported previously that *SMAD1* is aberrantly silenced in >85% of 259 examined DLBCL patients,[19] we queried the publicly available Cancer Cell Line Encyclopedia (CCLE) database for more evidence. Of the 1457 cell lines from ~40 tumor entities for which transcriptomic data based on RNA sequencing were available, the 18 DLBCL cell lines showed the lowest mean expression of SMAD1 (Figure 1A). Interestingly, the same 18 cell lines showed the highest level of *SMAD1* methylation (Figure 1B); SMAD1 expression and methylation of the *SMAD1* locus were strongly inversely correlated in these 18 cell lines (Figure 1C). Two other SMAD proteins with strong homology to SMAD1, which have been implicated as acting in concert with SMAD1 to transactivate target genes of the TGF-β signaling pathway, were strongly expressed across all cell lines with no evidence of DNA methylation (SMAD5) or were not expressed, but inconspicuous, relative to other tumor entities (SMAD9; supplemental Figure 1A-D). Other common types of lymphoma (Burkitt, Hodgkin) showed very different SMAD1 expression and methylation patterns, with generally higher SMAD1 expression and less evidence for methylation (supplemental Figure 1A-D).

We next experimentally addressed a possible inverse correlation between SMAD1 expression and *SMAD1* methylation in a panel of 11 DLBCL cell lines covering GCB and ABC subtypes. Only 1 of the 11 cell lines showed evidence of SMAD1 expression, as determined by western blotting (Figure 1D). Interestingly, bisulfite sequencing of 5 regions enriched for CG dinucleotides in the *SMAD1* promoter (supplemental Figure 1F) that had previously been identified as being subject to hypermethylation[21] revealed that the $SMAD1^+$ cell line SU-DHL-6 exhibited a lower mean methylation level compared with 3 $SMAD1^-$ cell lines across these 5 regions (Figure 1E). Regions 2 and 4 differed most markedly in terms of their methylation (Figure 1E). We next assessed SMAD1 expression and *SMAD1* methylation status of 6 primary patient cases of DLBCL from various sites (testis, lung, lymph nodes) by immunohistochemistry and bisulfite sequencing, respectively. All 6 DLBCL cases (1 was classified as GCB and 5 were classified as a non-GCB subtype according to the Hans algorithm)[20] were negative for SMAD1 (representative photomicrographs, Figure 2A), irrespective of their tissue of origin, and they exhibited strong methylation of region 2 (Figure 2B) and of the other 4 regions examined (supplemental Figure 2A). Two marginal zone B-cell lymphomas of the stomach that were analyzed alongside the DLBCL cases showed similar methylation patterns as the DLBCL cases; in contrast, the *SMAD1* promoter region 2 of immunomagnetically isolated B cells from donor blood was unmethylated, as was region 2 in 3 normal lymph node samples (Figure 2B). The other regions differed less with regard to their methylation status (supplemental Figure 2A). GCB cells in lymph node sections were positive for SMAD1, as judged by immunohistochemistry (Figure 2A), as were normal B cells, as determined by western blotting (supplemental Figure 2B). The combined observations obtained by immunohistochemistry of 259 patients, as reported previously,[19] by mining of the CCLE database for paired methylation and expression data for all available DLBCL and Hodgkin and Burkitt lymphoma cell lines, and by methylation and expression analyses of 6 primary DLBCL samples, several cell lines, and normal control samples suggest that SMAD1 is recurrently silenced by methylation of its promoter region in DLBCL but not in other lymphomas or normal B cells.

SMAD1 expression and susceptibility to TGF-β–induced apoptosis are restored by DAC treatment

We next addressed whether the inhibition of de novo DNA methylation by exposure to the cytidine analog DAC, which efficiently inhibits the

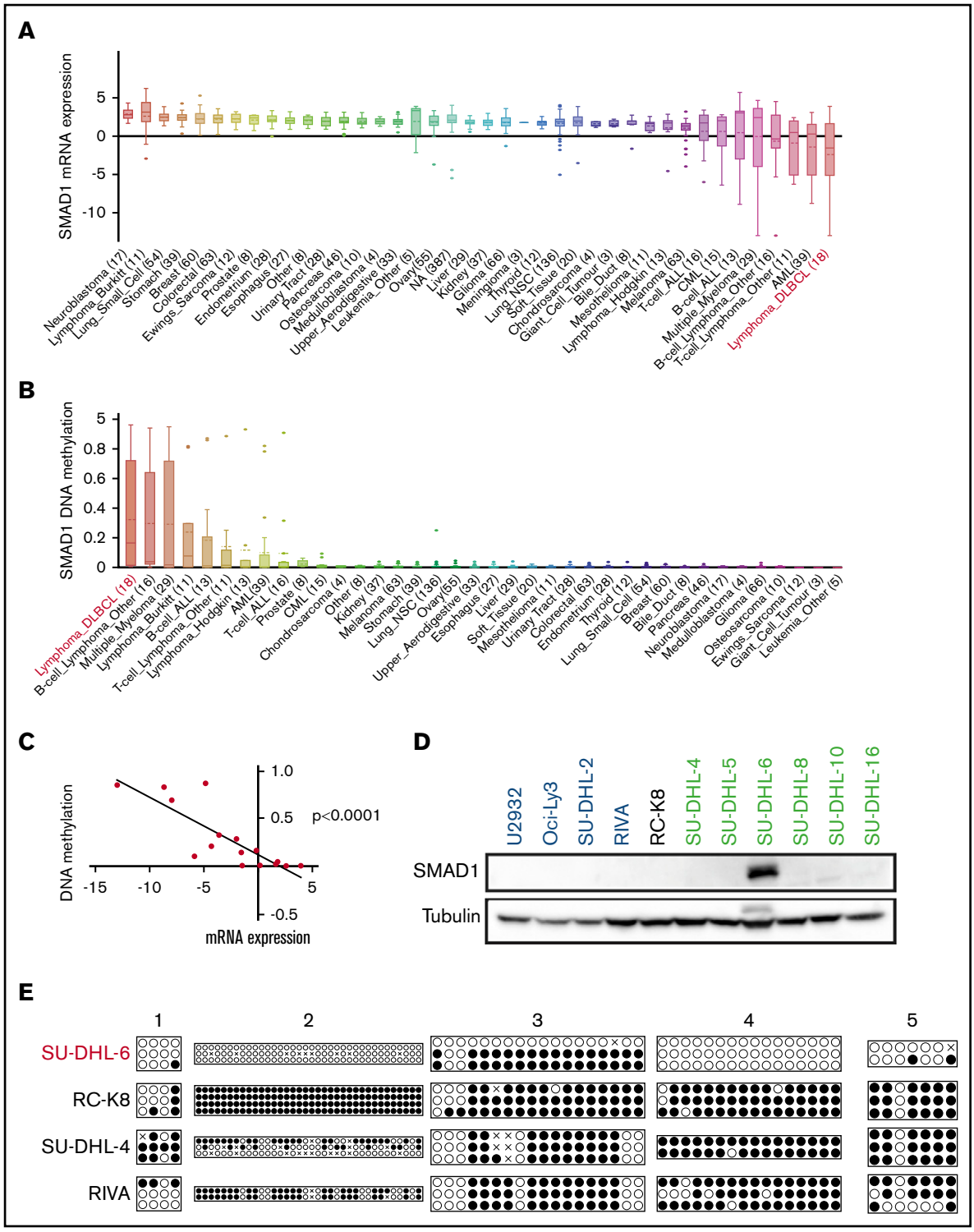

Figure 1. SMAD1 is silenced by DNA methylation of its promoter region in the majority of DLBCL cell lines. In silico analysis of ~1000 cell lines of the various indicated origins that are publicly available through the CCLE database with respect to SMAD1 expression (A) and SMAD1 gene methylation (B). DLBCL cell lines are highlighted in red. (C) Correlation between SMAD1 expression and gene methylation in DLBCL cell lines in the CCLE database. (D) SMAD1 expression, as determined by western blotting of a panel of DLBCL cell lines. ABC DLBCL cell lines are in blue, and GCB DLBCL cell lines are in green. The classification of RC-K8 is controversial. Tubulin serves as loading control. (E) Methylation analysis by bisulfite sequencing of 5 regions of the *SMAD1* promoter in SMAD1-expressing (SU-DHL-6) vs SMAD1^{-} (RC-K8, SU-DHL-4, RIVA) cell lines, as determined by bisulfite sequencing. Each circle represents 1 CG dinucleotide. Each line represents 1 clone. Two to 4 clones were sequenced per sample. ●, methylated cytosine; ○, unmethylated cytosine; ×, aligned mismatches between genomic and bisulfite sequences.

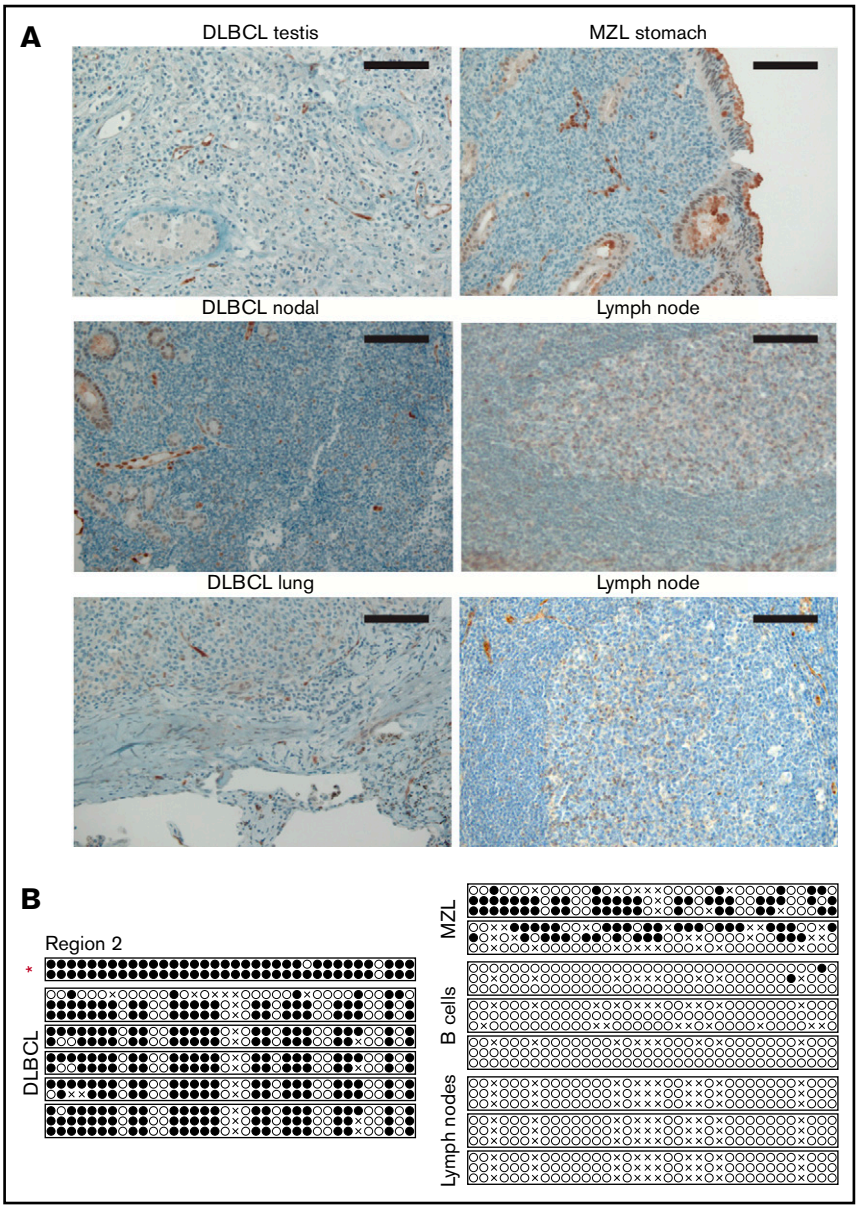

Figure 2. DLBCL patient samples exhibit low SMAD1 expression and high *SMAD1* promoter hypermethylation. (A) Immunohistochemical SMAD1 staining of DLBCL patient samples derived from testis, lung, and lymph nodes, as well as a gastric marginal zone lymphoma (MZL) sample. Normal lymph nodes are shown as control. Scale bars, 100 μm. (B) Methylation analysis by bisulfite sequencing of region 2 within the *SMAD1* promoter in DLBCL, MZL, normal B-cell, and lymph node samples. Each circle represents 1 CG dinucleotide. Each line represents 1 clone. Two or 3 clones were sequenced per sample. ●, methylated cytosine; ○, unmethylated cytosine; ×, aligned mismatches between genomic and bisulfite sequences. The red asterisk marks the patient sample that was further used for patient-derived xenotransplantation experiments in Figure 6.

methyltransferase DNMT3, would restore SMAD1 expression in SMAD1$^-$ DLBCL cell lines. Indeed, 4 days of exposure were sufficient to restore SMAD1 transcription and protein expression in a subset of our initially SMAD1$^-$ cell lines to roughly the level observed in the SMAD1$^+$ cell line SU-DHL-6, as determined by qRT-PCR and western blotting (Figure 3A-B). SMAD1$^+$ SU-DHL-6 cells did not respond to DAC with (even) higher SMAD1 expression (Figure 3A-B). Other cell lines that were initially SMAD1$^-$ failed to respond to DAC with SMAD1 reactivation, as judged by qRT-PCR and western blotting (supplemental Figure 3A-B). In those cell lines that responded to DAC, increased SMAD1 expression correlated with increased expression of the recently identified SMAD1 target S1PR2 (Figure 3C); in contrast, only 1 of the 4 cell lines that failed to upregulate SMAD1 at the protein level upon DAC exposure exhibited increased expression of S1PR2 (supplemental Figure 3C). Interestingly, genomic editing of the first exon of *SMAD1* in 1 of the DAC-responsive cell lines, SU-DHL-4, abrogated the reactivation of SMAD1 upon DAC exposure (Figure 3D; supplemental Figure 3D), as well as the induction of S1PR2 expression upon treatment with DAC, especially in combination with the S1PR2 inducer TGF-β (Figure 3E). Because we had previously shown that S1PR2 expression induced by TGF-β signaling promotes DLBCL apoptosis, we subjected the SMAD1$^-$ and DAC-responsive cell lines RIVA, SU-DHL-4, and RC-K8 to DAC treatment, with and without additional exposure to TGF-β; the SMAD1$^+$ cell line SU-DHL-6 served as control. As reported, TGF-β robustly induced S1PR2 expression,[19] which was further enhanced by prior DNA demethylation in all SMAD1$^-$ cell lines, but not in the SMAD1$^+$ cell line SU-DHL-6 (supplemental Figure 3E), and coincided with apoptosis induction, as determined by annexin V staining (supplemental Figure 3F). TGF-β–induced apoptosis was enhanced by prior DNA demethylation in DAC-responsive cell lines, as well as in SU-DHL-6 cells, which constitutively express SMAD1, indicating that the SMAD1/S1PR2 axis represents 1 of multiple pathways to

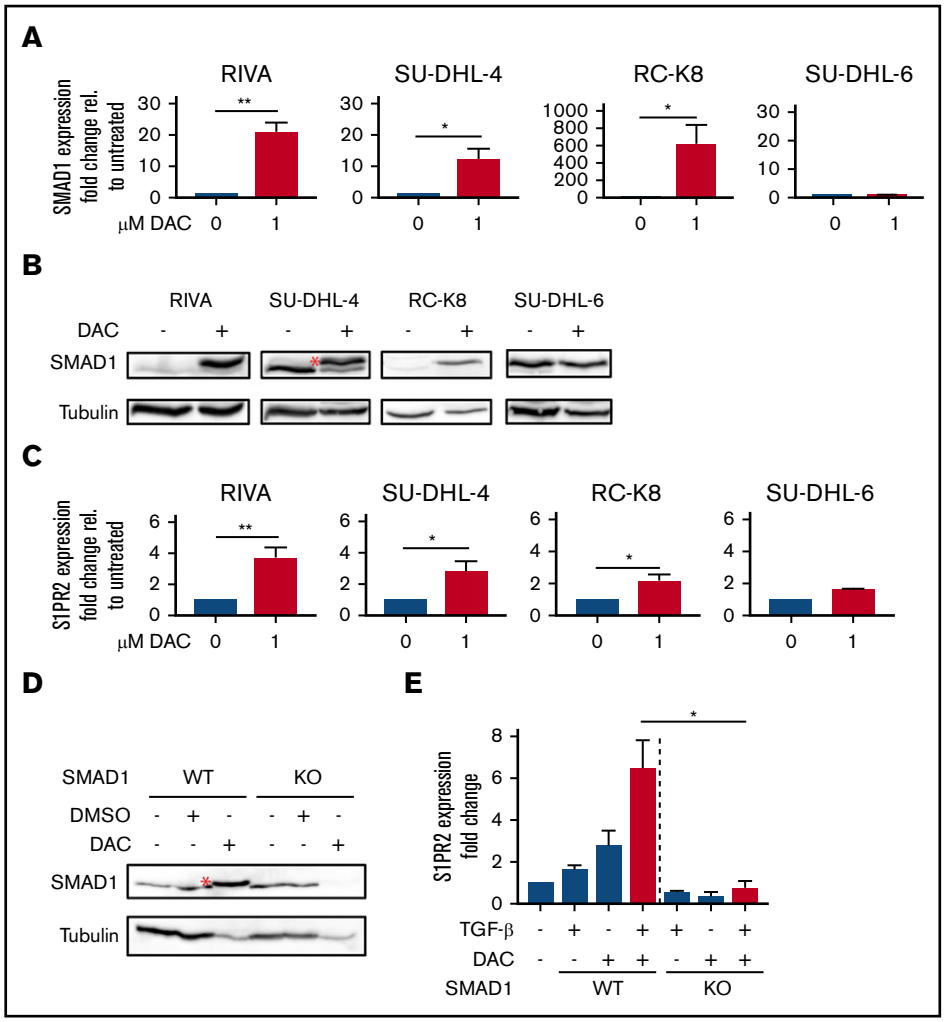

Figure 3. SMAD1 expression is restored by DAC treatment. SMAD1 expression at the transcript (A) and protein (B) levels after DAC treatment (1 μM for 96 hours) of 4 DLBCL cell lines, as determined by qRT-PCR and western blotting. (A) Results from 4 (RIVA, SU-DHL-4, and RC-K8) and 2 (SU-DHL-6) independent experiments are pooled. SU-DHL-6 cells express SMAD1 prior to DAC treatment; all other cell lines are initially (pre-DAC) SMAD1^{-}. (C) S1PR2 expression at the messenger RNA level after 1 μM DAC treatment (1 μM for 96 hours) of the cell lines in panel A. Pooled results from 4 (RIVA, SU-DHL-4 and RC-K8) and 2 (SU-DHL-6) independent experiments are shown. (D) SMAD1 expression of SMAD1^{WT} and SMAD1^{KO} SU-DHL-4 cells after exposure to DAC or vehicle control. The red asterisks (*) in panels B and D mark the correct band corresponding to SMAD1. Note that in SU-DHL-4 cells, and to a lesser extent in RIVA and RC-K8 cells (B), our SMAD1 antibody recognizes a second faster migrating band that is not SMAD1, because it is not lost in SMAD1^{KO} SU-DHL-4 cells, and that goes away upon DAC treatment. (E) Relative S1PR2 expression, as determined by qRT-PCR, of SMAD1^{WT} and SMAD1^{KO} SU-DHL-4 cells after DAC (1 μM for 96 hours) and TGF-β (2 ng/mL for 24 hours) treatment. Pooled results from 3 independent experiments are shown. Bar graphs show mean + SEM. *$P < .05$, **$P < .01$, Student *t* test.

TGF-β–induced cell death (supplemental Figure 3F). This observation was confirmed in SMAD1-knockout (SMAD1^{KO}) SU-DHL-4 cells, which were killed effectively in vitro by combined DAC/TGF-β exposure, despite failing to express SMAD1 and S1PR2 (Figure 3D-E; supplemental Figure 3G). The combined results suggest that SMAD1 is epigenetically silenced by DNA methylation in a subset of DLBCL cell lines, which favors cell survival in the presence of TGF-β; this aberrant regulation can be reversed by pharmacological DNA demethylation.

DAC treatment decreases the tumor burden in vivo in subcutaneous and orthotopic models of DLBCL

We have previously reported that clones of the SMAD1-expressing cell line SU-DHL-6 that have been genome edited to knock out *SMAD1* engraft better in the spleen and bone marrow of humanized mice than do WT clones.[19] The mouse strain that served as host strain for orthotopic growth was generated on the Rag2$^{-/-}$IL2Rγ$^{-/-}$ background, and it expresses the human cytokines macrophage colony-stimulating factor, interleukin-3, thrombopoietin, and granulocyte-macrophage colony-stimulating factor, as well as SIRP1α from the respective murine loci (MISTRG).[13] This in vivo orthotopic growth advantage of SMAD1^{KO} SU-DHL-6 clones in MISTRG mice could be confirmed by comparative IVIS of WT SMAD1 (SMAD1^{WT}) and SMAD1^{KO} clones that had been lentivirally transduced with a luciferase expression construct (supplemental Figure 4A-C). To determine whether the restoration of SMAD1 expression that can be achieved by DAC treatment in vitro (Figure 3A-B) would reduce tumor growth

in vivo, we subcutaneously transplanted the SMAD1^{-} cell lines RC-K8 and SU-DHL-4 onto the flanks of NSG mice. DAC treatment significantly reduced, and even reversed, tumor growth over time in both cell lines when administered at 2 concentrations in a therapeutic setting (ie, once tumors were palpable) (Figure 4A-D). Tumor size and volume were significantly lower in DAC-treated mice at the study end point (Figure 4B,D). To be able to investigate the effects of DAC in an orthotopic model, we took advantage of MISTRG and MISTRG6 mice, which differ from the parental MISTRG strain in their additional expression of human interleukin-6 from a knock-in allele.[14] Although MISTRG mice efficiently supported the orthotopic engraftment of SU-DHL-4 cells (delivered IV), we had to resort to MISTRG6 mice for the orthotopic (IV) xenotransplantation of RC-K8 cells. Their luciferase expression allowed for the visualization and detection of SU-DHL-4 and RC-K8 cells by IVIS in the hip and leg bones as early as 2 weeks postinjection (Figure 4E; supplemental Figure 4D-E). In vehicle-treated mice, the tumor burden increased over time as cells spread to various internal organs over the 5-week (RC-K8) to 6-week (SU-DHL-4) time course; mice began to develop symptoms, such as weight loss and hind leg paralysis, at ~30 days posttumor cell injection (Figure 4E-G; supplemental Figure 4D-F). The development of clinical symptoms correlated well with a particularly high tumor burden, as determined by IVIS. In contrast, mice that had been administered daily doses of DAC starting at 14 days posttumor cell injection exhibited a stabilization of their tumor burden and did not develop overt disease symptoms (Figure 4E-G; supplemental Figure 4D-F). The combined results indicate that DAC reduces and reverses the growth of established DLBCL cell lines with aberrantly low or absent SMAD1 expression resulting from promoter hypermethylation in ectopic and orthotopic models.

The success of DAC treatment requires SMAD1 reactivation in vivo in subcutaneous and orthotopic models

To examine whether the beneficial effects of DAC treatment in vivo require SMAD1, we compared SMAD1-proficient and SMAD1-deficient SU-DHL-4 cells in terms of their growth kinetics in the subcutaneous tumor model described in Figure 4. To this end, NSG mice were subcutaneously transplanted with SMAD1^{WT} and SMAD1^{KO} SU-DHL-4 cells in their left and right flanks, respectively, and subjected to DAC or vehicle treatment once tumors were palpable. Although SMAD1^{WT} cells showed the usual rapid response to DAC that is characterized by slowing of tumor growth and tumor regression, this was not the case with SMAD1^{KO} cells (Figure 5A-B). Similar observations were made in the orthotopic model, as determined by IVIS measurements over time (Figure 5C-D) and by monitoring disease symptoms (weight loss, hind leg paralysis) over time (Figure 5E). The combined results indicate that the therapeutic success of DAC requires a functional *SMAD1* locus and rules out a major contribution of other differentially methylated genes to tumor suppression induced by demethylating agents.

Primary DLBCL cells with low SMAD1 expression and high *SMAD1* promoter hypermethylation engraft in MISTRG6 mice and are responsive to DAC treatment

Because MISTRG6 mice support the orthotopic growth of DLBCL cell lines, we speculated that the same strain might also allow us to develop a patient-derived xenograft model that would lend itself to preclinical testing of DAC efficacy. We obtained live cells from a bone marrow biopsy from a patient with stage IVBE ABC DLBCL with extranodal manifestations in the liver, an International Prognostic Index score of 5, splenomegaly, and ~7% tumor cell infiltration of the marrow that exhibited high *SMAD1* methylation in 4 of the 5 investigated regions (Figure 2B; supplemental Figure 2A, marked by an asterisk) and no detectable SMAD1 or S1PR2 expression at the RNA level (Figure 6A). All available viable tumor cells (100 000) were injected IV into a MISTRG6 recipient, where they engrafted in the bone marrow and spleen within 6 weeks. Spleen cells from this mouse were serially transplanted IV into larger cohorts of MISTRG6 mice and subjected to daily DAC or vehicle (PBS) treatment throughout the 5-week course of the experiment. The serially transplanted primary DLBCL cells formed splenic lymphomas with bone marrow involvement that were highly responsive to DAC treatment, as judged by flow cytometric quantification of human cells in the spleen and bone marrow, as well as by determining spleen weights at the study end point (Figure 6B-E). Cells residing in the bone marrow were more resistant to DAC than were those in the spleen (Figure 6B-D). Spleens of mice that had been subjected to DAC treatment exhibited less tumor cell infiltration, as judged by histology (Figure 6F), and a generally stronger SMAD1 signal (Figure 6G). The combined results suggest that primary DLBCL cells can engraft in the spleen and bone marrow of MISTRG6 mice and that DAC treatment reduces the tumor burden associated with primary DLBCL xenotransplantation in this model.

Discussion

Genes encoding epigenetic modifiers, and especially those encoding histone-modifying enzymes, such as HMTs or histone acetyltransferases, are among the most recurrently mutated genes in DLBCL,[11] and perturbations of the epigenome are increasingly recognized as a driving force in DLBCL pathogenesis.[22] Both main subtypes of DLBCL are commonly affected by loss-of-function mutations of the HMT *KMT2D*, gain-of-function mutations of the HMT *EZH2*, and loss-of-function mutations of the histone acetyltransferases *CREBBP* and *EP300*, which together occur in ~50% of DLBCL patients.[11] Mutations in epigenetic modifiers are believed to be founder events that predispose normal B cells to malignant transformation.[22] In the panel of 11 cell lines investigated in this study with respect to SMAD1 methylation and expression, mutations in the 4 above-mentioned genes were even more common than in published patient cohorts, with *CREBBP/EP300* mutations together affecting 9 of 11 cell lines[23] and *EZH2/KMT2D* mutations affecting 4 of 11 cell lines.[24] Repressive histone marks, and especially the polycomb-mediated methylation on Lys27 of histone H3, have been directly linked to aberrant hypermethylation of CpG islands in cancer cells.[14-16] We and other investigators have performed genome-wide DNA methylation profiling of DLBCL cell lines and primary patient material, which has led to the identification of numerous genes that are aberrantly silenced in both subtypes of DLBCL.[7,8] Examples of tumor-suppressor genes known to be silenced by promoter hypermethylation in DLBCL include *DUSP4*, *MGMT*, *CDKN2A*, and the lamin A/C gene.[7,25-27] Epigenetic heterogeneity has emerged as an important hallmark of DLBCL, and a high degree of inter- and intratumoral heterogeneity has been associated directly with disease aggressiveness, likelihood of relapse, and inferior patient survival.[28-30]

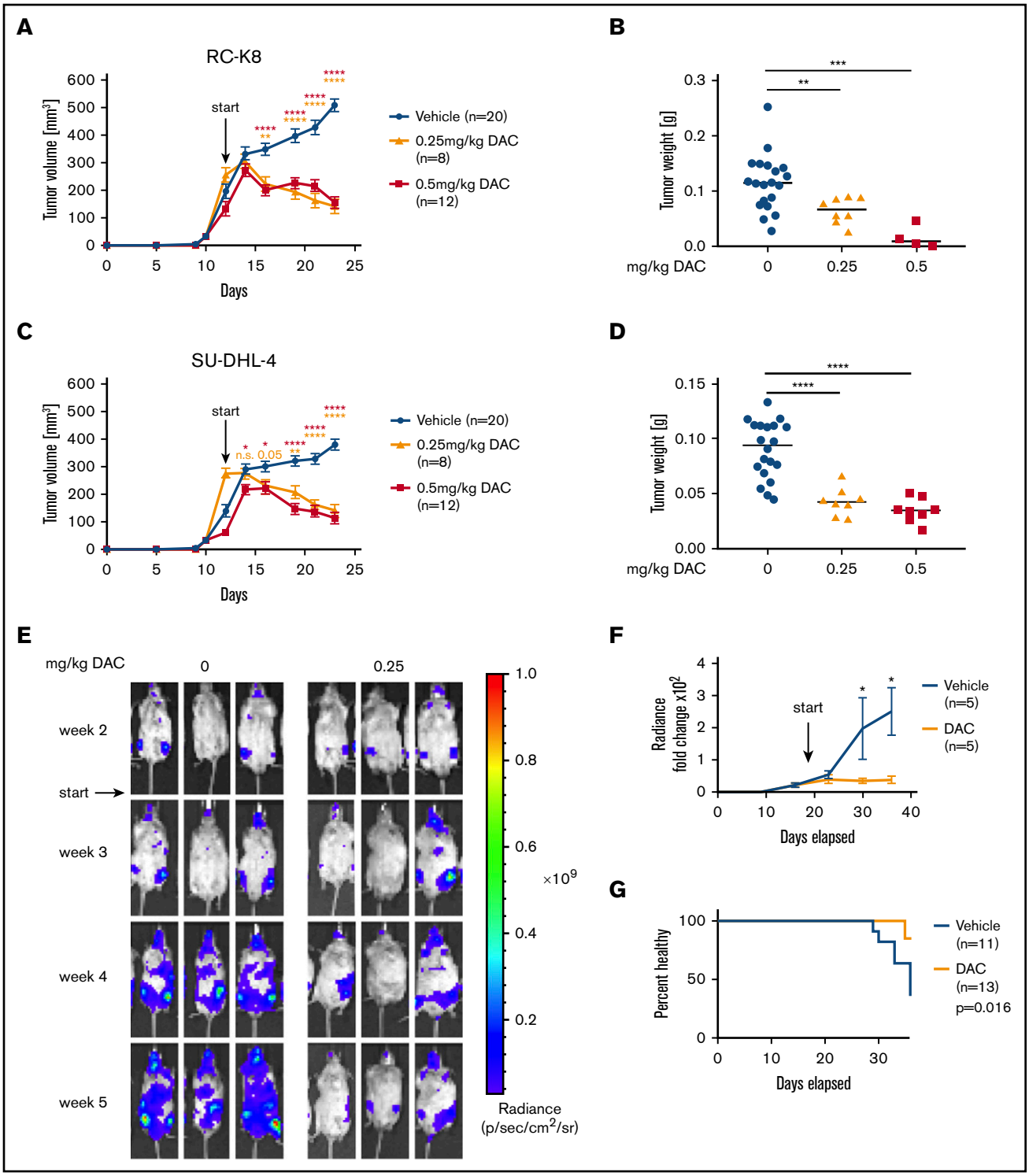

Figure 4. DAC treatment decreases tumor burden in vivo in a subcutaneous and in a novel orthotopic model of DLBCL RC-K8 (A-B) and SU-DHL-4 (C-D) DLBCL cell lines were subcutaneously injected into the flanks of NSG mice. From day 12 after transplantation, mice were treated systemically with 0.25 mg/kg or 0.5 mg/kg DAC for 2 cycles, 5 days per week. Tumor volume was measured continuously (A,C), and tumor weight was measured at the end point (B,D). (B,D) Because of the toxicity of the 0.5-mg/kg treatment, only 4 of 12 mice and 8 of 12 mice are represented for RC-K8 and SU-DHL-4, respectively, at the end point. Graphs in panels A and C show mean ± SEM; in panels B and D, median values are presented as horizontal lines. Graphs represent pooled data from 2 independent experiments. The *P* values were calculated using the Mann-Whitney *U* test. (E-G) RC-K8 cells were subjected to lentiviral gene transfer of luciferase and injected IV into MISTRG6 mice. Mice were treated with 0 or 0.25 mg/kg DAC starting from day 19 after injection. Representative IVIS images of mice (E) and the radiance over 5 weeks (F) are shown. Results in panel F are from 1 experiment and representative of 2 independent ones. (G) Survival curve showing the percentage of injected mice without symptoms of disease (paralysis, weight loss); the *P* value was calculated using the log-rank (Mantel-Cox) test. Data are pooled from 2 independent experiments. *$P < .05$, **$P < .01$, ***$P < .001$, ****$P < .0001$. n.s., not significant.

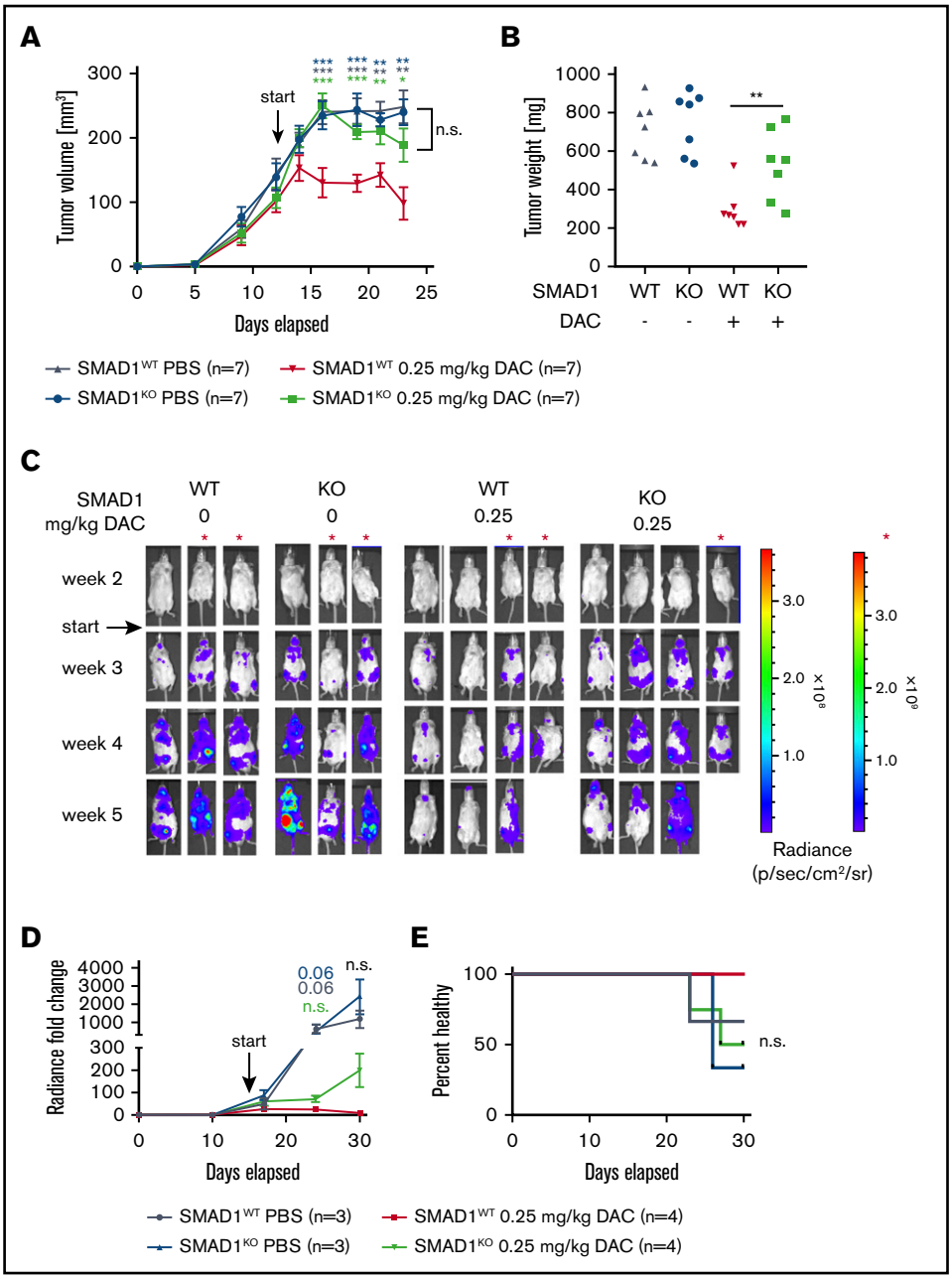

Figure 5. A functional *SMAD1* locus is required for the therapeutic efficacy of DAC treatment. (A-B) SMAD1^{WT} and SMAD1^{KO} SU-DHL-4 cells were injected subcutaneously into the flanks of NSG mice. From day 12 after transplantation, mice were treated systemically with 0.25 mg/kg DAC for 2 cycles, 5 days per week. The tumor volume was measured continuously (A), and tumor weights were recorded at the end point (B). Data in panels A-B are pooled from 2 independent studies, and *P* values were calculated using the Mann-Whitney *U* test (for every time point relative to the red curve in panel A). (C-E) SMAD1^{WT} and SMAD1^{KO} SU-DHL-4 cells were subjected to lentiviral gene transfer of luciferase and injected IV into MISTRG mice. Mice were treated with 0 or 0.25 mg/kg DAC starting from day 15 after injection. IVIS images of all included mice (C) and the radiance over 5 weeks (D) are shown. (D) *P* values were calculated using the Mann-Whitney *U* test (for every time point relative to the red curve). (E) Survival curve showing the percentage of injected mice without symptoms of disease (paralysis, weight loss). The log-rank (Mantel-Cox) test was used for statistical comparisons. Data in panels C-E are pooled from 2 studies; the scale marked with a red asterisk (*) (far right panel in panel C) applies to the mice denoted by the asterisk (*) in panel C. Differences in panels D-E show trends only; 1 mouse (KO, on DAC) died from its disease before the study end point, and 1 mouse (WT, on DAC) died from nondisease-related causes. $^{*}P < .05$, $^{**}P < .01$, $^{***}P < .001$.

Here, we provide experimental evidence for aberrant silencing of *SMAD1* by hypermethylation of 5 regions that are up- and downstream of the transcription start site; these *SMAD1* sites were previously identified in a study alongside 8 other loci as being recurrently hypermethylated in chemoresistant DLBCL and as being functionally required for chemosensitization.[21] One region, region 2, emerges from our analyses as possibly being more relevant than the other 4 in directing SMAD1 expression. Our data suggest that *SMAD1* is not hypermethylated solely as a consequence of exposure to chemotherapy; rather, data obtained from patient samples taken at diagnosis indicate that *SMAD1* silencing by promoter hypermethylation is a common, and probably early, event in DLBCL pathogenesis. We have previously examined the expression of SMAD1 by immunohistochemistry in 2 large patient cohorts and found that only 7 of 75 patients in 1 cohort (9.3%) and 29 of 184 patients in the other cohort (15.7%) had tumor cells that expressed SMAD1 (range, 10%-90% of tumor cells being positive), whereas B cells from peripheral blood or GCB cells in normal tonsils were invariably positive for SMAD1.[19] The fraction of SMAD1^{+} cases was equally low in patients with GCB (15%) or ABC (13%) DLBCL subtypes, indicating that SMAD1 is selectively downregulated, irrespective of the subtype.[19] Our data contrast to some degree with another survey of SMAD1 expression that also used immunohistochemistry of tissue microarrays but was conducted with an antibody specific for the phosphorylated forms of SMAD1 and SMAD5.[21] This study concluded that the majority (70%) of the examined 248 DLBCL cases showed phospho-SMAD expression in ≥20% of the tumor cells.[21] The different specificities

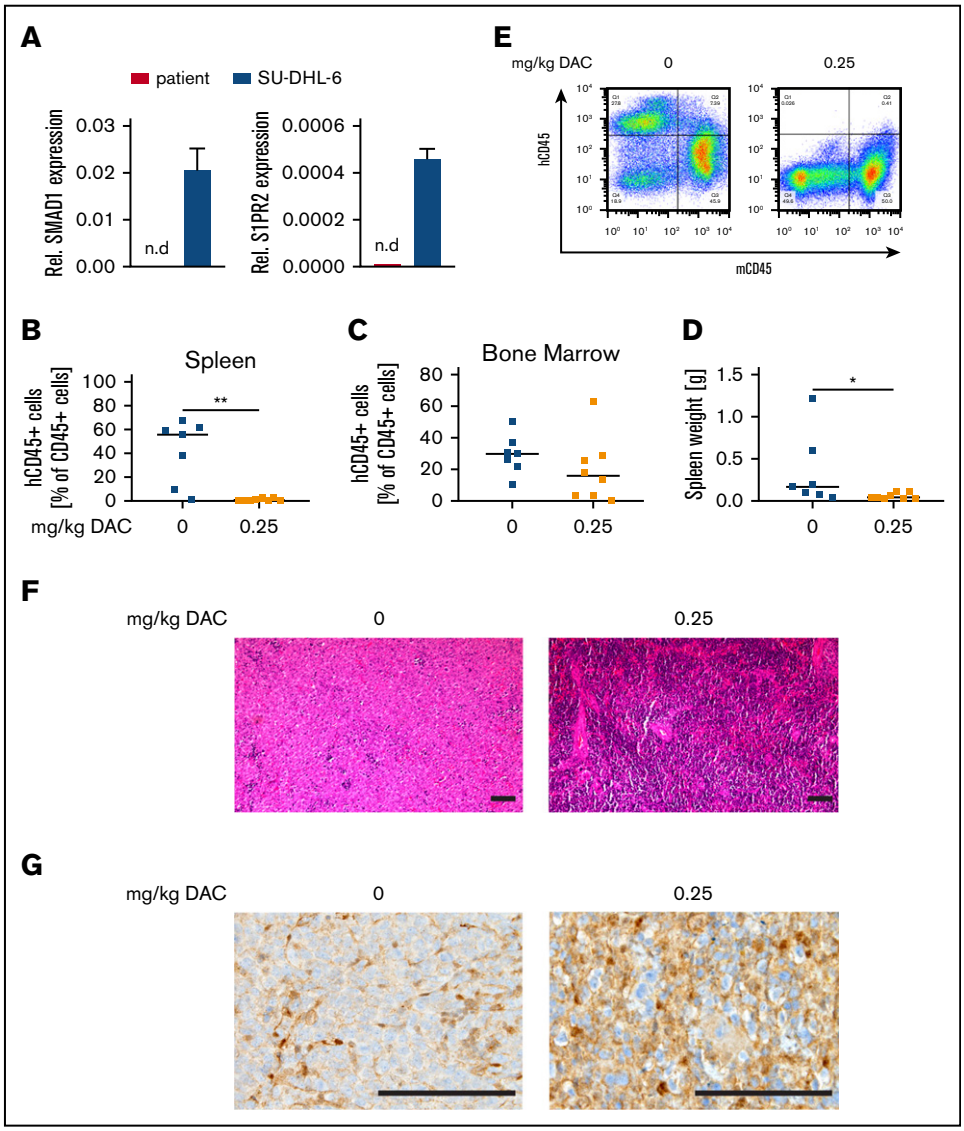

Figure 6. SMAD1^{-}DLBCL patient cells respond to DAC treatment in a patient-derived xenograft model. (A) SMAD1 and S1PR2 expression in CD19^{+} primary DLBCL cells, as determined by qRT-PCR; SU-DHL-6 cells are shown as positive control. Percentages of human CD45^{+} cells in the spleen (B) and bone marrow (C) of MISTRG6 mice that were injected with primary DLBCL cells and treated with 0.25 mg/kg DAC for 3 cycles of 5 days per week. (D) Spleen weights at the end point. (E) Representative FACS plots showing frequencies of human and mouse CD45^{+} cells in the spleens. In panels B-D, each symbol represents 1 mouse and horizontal lines represent median values; data are pooled from 3 independent experiments. (F) Hematoxylin and eosin–stained sections of spleens from representative mice treated or not with DAC. Scale bars, 100 μm. (G) SMAD1 immunohistochemical staining of representative mice treated or not with DAC. Scale bars, 100 μm. *$P < .05$, **$P < .01$, Mann-Whitney *U* test. n.d., not detectable.

of the antibodies used likely account for the observed differences in SMAD1 expression/phosphorylation in the 2 datasets. Bisulfite sequencing is labor intensive and cannot readily be scaled up to examine large numbers of patients; however, the small number of patients for whom both high-quality DNA (for *SMAD1* bisulfite sequencing) and histological sections (for SMAD1 immunohistochemistry) were available suggests that aberrant SMAD1 silencing is attributable to *SMAD1* hypermethylation. This was also confirmed in in silico analyses of 18 DLBCL cell lines included in the CCLE database and in our own panel of DLBCL cell lines. In contrast, in the above-mentioned study published by Clozel et al,[21] the frequency of *SMAD1*-hypermethylated cases was found to be substantially lower (75% of patients with DLBCL showed ≤5% *SMAD1* methylation) than in our small patient cohort available for methylation and expression analysis; furthermore, the investigators found a clear bias of *SMAD1* methylation toward the ABC DLBCL subtype in their cohort. Because our small patient selection was strongly biased toward ABC DLBCL, we may be overestimating the role of *SMAD1* methylation in the silencing of the locus.

SMAD1 relays signals downstream of the TGF-β receptor and becomes phosphorylated upon ligand binding. Among the target genes of the TGF-βRII/SMAD1 axis is the gene encoding the G protein–coupled receptor S1PR2, which we have recently identified by chromatin immunoprecipitation.[19] The genes encoding S1PR2 and its downstream adaptor protein Gα13, *GNA13*, are known to be recurrently mutated in the GCB subtype of DLBCL.[17] In contrast, in ABC DLBCL, the expression of S1PR2 is silenced by overexpression of FOXP1, a transcriptional repressor of *S1PR2* that binds to 2 genomic loci that overlap with the SMAD1 binding sites in the 5-kb regulatory region upstream of the *S1PR2* transcription start site.[18] The new data presented here show that, in most cases of DLBCL, an additional epigenetic layer of regulation is in place that prevents S1PR2 expression (Figure 7). The mechanistic basis for the tumor-suppressive properties of S1PR2 and its Gα13-driven downstream signaling pathway are not fully understood, although gain-of-function and loss-of-function experiments have confirmed their critical contribution to DLBCL pathogenesis. Evidence for this has come from xenotransplantation settings, in which the loss of *S1PR2* contributes to tumor growth in

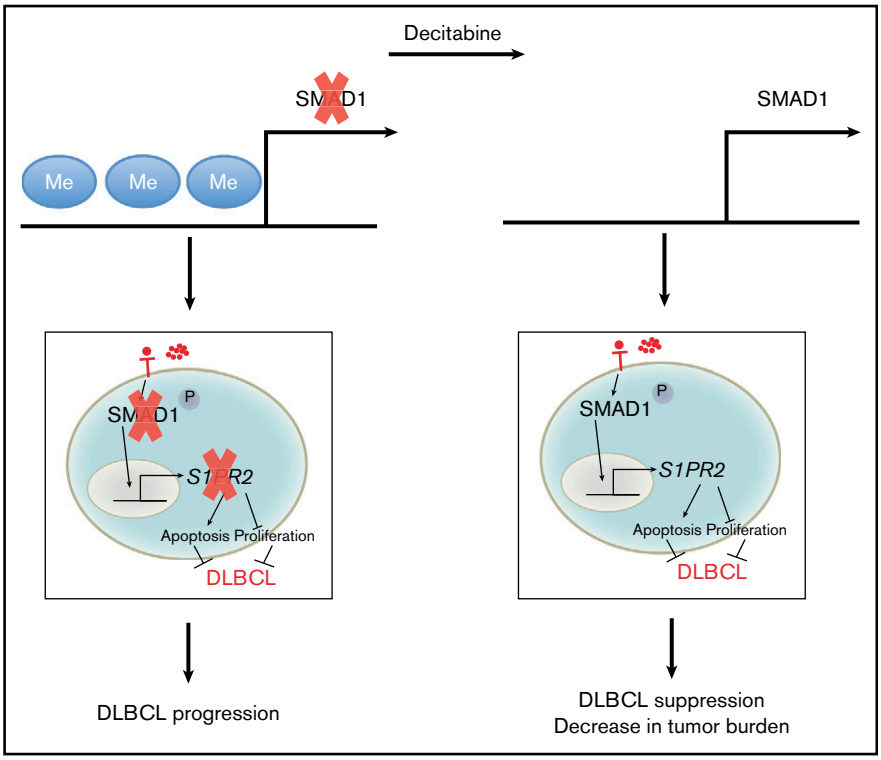

Figure 7. Schematic summary of the dysregulation of SMAD1 expression by promoter hypermethylation and the consequences for DLBCL survival and growth. In both subtypes of DLBCL, the promoter region of *SMAD1* is recurrently hypermethylated, which causes *SMAD1* gene repression. Repression of SMAD1 blocks the tumor-suppressive TGF-β/SMAD1/S1PR2 pathway. Loss of S1PR2 expression within the germinal center promotes B-cell proliferation and prevents S1P-driven apoptosis. DAC demethylates *SMAD1* and restores SMAD1 expression, allowing its phosphorylation upon TGF-β binding and its translocation into the nucleus, followed by S1PR2 expression, as well as a reduction in the tumor burden in experimental settings.

ectopic and orthotopic models, as well as from models of MYC-driven lymphomagenesis, which is accelerated in mice that are deficient for S1pr2.[18,19]

Our results provide experimental evidence from ectopic and orthotopic xenotransplantation models, using cell lines and primary cells, that DAC or other inhibitors of de novo DNA methylation might be beneficial in DLBCL, especially in patients with low or no SMAD1 expression. Similar effects have been shown previously for the relatively chemoresistant DLBCL cell line Oci-Ly7; DAC alone, and especially in synergy with doxorubicin, reduced subcutaneous tumor growth.[21] Another study by Kalac et al, using the cell line Oci-Ly1 in a subcutaneous model, found strong effects of DAC only in combination with the histone deacetylase inhibitor panobinostat.[31] DAC and its analog azacitidine are approved for the treatment of myelodysplastic syndromes and acute myeloid leukemias. Both compounds are comparatively well tolerated, and as monotherapy they yield response rates from 10% to 50% in these 2 indications; however, they are not curative.[32,33] The recent addition of the Bcl-2 inhibitor venetoclax to DAC or azacitidine increased complete remission rates for acute myeloid leukemias in the high-risk elderly to >60%.[34] Azacitidine priming, followed by standard chemo-immunotherapy, in 10 high-risk patients with newly diagnosed DLBCL has already shown some promise in a phase I clinical trial.[21] Our data indicate that this strategy deserves further attention, and we propose loss of SMAD1 expression as a potentially useful biomarker in rationally guiding treatment decisions. Our results further highlight the value of MISTRG and MISTRG6 mice as host strains for pre- or coclinical testing of novel drugs or of drug combinations. We show here that primary DLBCL cells can be expanded and serially passaged in MISTRG6 mice to generate a disease model that offers a window of opportunity for therapeutic testing of ~4 to 6 weeks. Our immunohistochemical staining suggests that SMAD1 expression is at least partially restored by DAC treatment in the primary xenotransplantation setting, providing the first hints that the success of this treatment may be linked to SMAD1 restoration. The combined results lend further support to the concept that epigenetic modifications leading to aberrant silencing of key tumor suppressors in DLBCL can be targeted pharmacologically with approved and well-tolerated agents.

Acknowledgments

The authors thank all consortium members of the Clinical Research Priority Program for support and helpful discussions, as well as Michael Bauer for help with cell sorting.

This work was supported by Swiss Cancer League grants KLS-3612-02-2015 and KFS-4120-02-2017 (A.M.). Additional support was provided by the Clinical Research Priority Program "Human Hemato-lymphatic Diseases" of the University of Zurich. A.S. was funded by the Forschungskredit of the University of Zurich.

Authorship

Contribution: A.S. designed, performed, and analyzed experiments and cowrote the manuscript; C.-T.W. performed and analyzed experiments; H.H. and K.B. helped with experiments and provided critical tools and advice; A.P.A.T. and M.G.M. provided critical tools and patient samples; A.T. provided, stained, and analyzed patient samples; and A.M. supervised the study and cowrote the manuscript.

Conflict-of-interest disclosure: The authors declare no competing financial interests.

ORCID profile: H.H., 0000-0002-8078-6570.

Correspondence: Anne Müller, Institute of Molecular Cancer Research, University of Zurich, Winterthurerstr 180, 8057 Zurich, Switzerland; e-mail: mueller@imcr.uzh.ch.

References

1. Chapuy B, Stewart C, Dunford AJ, et al. Molecular subtypes of diffuse large B cell lymphoma are associated with distinct pathogenic mechanisms and outcomes [published corrections appear in *Nat. Med*. 2018;24(8):1290-1291; *Nat. Med*. 2018;24(8):1292]. *Nat Med*. 2018;24(5):679-690.
2. Schmitz R, Wright GW, Huang DW, et al. Genetics and pathogenesis of diffuse large B-cell lymphoma. *N Engl J Med*. 2018;378(15):1396-1407.
3. Alizadeh AA, Eisen MB, Davis RE, et al. Distinct types of diffuse large B-cell lymphoma identified by gene expression profiling. *Nature*. 2000;403(6769):503-511.
4. Rosenwald A, Wright G, Chan WC, et al; Lymphoma/Leukemia Molecular Profiling Project. The use of molecular profiling to predict survival after chemotherapy for diffuse large-B-cell lymphoma. *N Engl J Med*. 2002;346(25):1937-1947.
5. Phelan JD, Young RM, Webster DE, et al. A multiprotein supercomplex controlling oncogenic signalling in lymphoma. *Nature*. 2018;560(7718):387-391.
6. Bojarczuk K, Wienand K, Ryan JA, et al. Targeted inhibition of PI3Kα/δ is synergistic with BCL-2 blockade in genetically defined subtypes of DLBCL. *Blood*. 2019;133(1):70-80.
7. Schmid CA, Robinson MD, Scheifinger NA, et al. DUSP4 deficiency caused by promoter hypermethylation drives JNK signaling and tumor cell survival in diffuse large B cell lymphoma. *J Exp Med*. 2015;212(5):775-792.
8. Asmar F, Punj V, Christensen J, et al. Genome-wide profiling identifies a DNA methylation signature that associates with TET2 mutations in diffuse large B-cell lymphoma. *Haematologica*. 2013;98(12):1912-1920.
9. Pasqualucci L, Dalla-Favera R. The genetic landscape of diffuse large B-cell lymphoma. *Semin Hematol*. 2015;52(2):67-76.
10. Pasqualucci L, Dominguez-Sola D, Chiarenza A, et al. Inactivating mutations of acetyltransferase genes in B-cell lymphoma. *Nature*. 2011;471(7337):189-195.
11. Pasqualucci L, Trifonov V, Fabbri G, et al. Analysis of the coding genome of diffuse large B-cell lymphoma. *Nat Genet*. 2011;43(9):830-837.
12. Juskevicius D, Jucker D, Klingbiel D, Mamot C, Dirnhofer S, Tzankov A. Mutations of CREBBP and SOCS1 are independent prognostic factors in diffuse large B cell lymphoma: mutational analysis of the SAKK 38/07 prospective clinical trial cohort. *J Hematol Oncol*. 2017;10(1):70.
13. Zhang J, Vlasevska S, Wells VA, et al. The CREBBP acetyltransferase is a haploinsufficient tumor suppressor in B-cell lymphoma. *Cancer Discov*. 2017;7(3):322-337.
14. Schlesinger Y, Straussman R, Keshet I, et al. Polycomb-mediated methylation on Lys27 of histone H3 pre-marks genes for de novo methylation in cancer. *Nat Genet*. 2007;39(2):232-236.
15. Gao F, Ji G, Gao Z, et al. Direct ChIP-bisulfite sequencing reveals a role of H3K27me3 mediating aberrant hypermethylation of promoter CpG islands in cancer cells. *Genomics*. 2014;103(2-3):204-210.
16. Gal-Yam EN, Egger G, Iniguez L, et al. Frequent switching of polycomb repressive marks and DNA hypermethylation in the PC3 prostate cancer cell line. *Proc Natl Acad Sci USA*. 2008;105(35):12979-12984.
17. Muppidi JR, Schmitz R, Green JA, et al. Loss of signalling via Gα13 in germinal centre B-cell-derived lymphoma. *Nature*. 2014;516(7530):254-258.
18. Flori M, Schmid CA, Sumrall ET, et al. The hematopoietic oncoprotein FOXP1 promotes tumor cell survival in diffuse large B-cell lymphoma by repressing S1PR2 signaling. *Blood*. 2016;127(11):1438-1448.
19. Stelling A, Hashwah H, Bertram K, Manz MG, Tzankov A, Müller A. The tumor suppressive TGF-β/SMAD1/S1PR2 signaling axis is recurrently inactivated in diffuse large B-cell lymphoma. *Blood*. 2018;131(20):2235-2246.
20. Hans CP, Weisenburger DD, Greiner TC, et al. Confirmation of the molecular classification of diffuse large B-cell lymphoma by immunohistochemistry using a tissue microarray. *Blood*. 2004;103(1):275-282.
21. Clozel T, Yang S, Elstrom RL, et al. Mechanism-based epigenetic chemosensitization therapy of diffuse large B-cell lymphoma. *Cancer Discov*. 2013;3(9):1002-1019.
22. Jiang Y, Dominguez PM, Melnick AM. The many layers of epigenetic dysfunction in B-cell lymphomas. *Curr Opin Hematol*. 2016;23(4):377-384.
23. Hashwah H, Schmid CA, Kasser S, et al. Inactivation of CREBBP expands the germinal center B cell compartment, down-regulates MHCII expression and promotes DLBCL growth. *Proc Natl Acad Sci USA*. 2017;114(36):9701-9706.
24. Juskevicius D, Müller A, Hashwah H, Lundberg P, Tzankov A, Menter T. Characterization of the mutational profile of 11 diffuse large B-cell lymphoma cell lines. *Leuk Lymphoma*. 2018;59(7):1710-1716.
25. Martinez-Delgado B, Fernandez-Piqueras J, Garcia MJ, et al. Hypermethylation of a 5′ CpG island of p16 is a frequent event in non-Hodgkin's lymphoma. *Leukemia*. 1997;11(3):425-428.
26. Esteller M, Gaidano G, Goodman SN, et al. Hypermethylation of the DNA repair gene O(6)-methylguanine DNA methyltransferase and survival of patients with diffuse large B-cell lymphoma. *J Natl Cancer Inst*. 2002;94(1):26-32.
27. Agrelo R, Setien F, Espada J, et al. Inactivation of the lamin A/C gene by CpG island promoter hypermethylation in hematologic malignancies, and its association with poor survival in nodal diffuse large B-cell lymphoma. *J Clin Oncol*. 2005;23(17):3940-3947.
28. Chambwe N, Kormaksson M, Geng H, et al. Variability in DNA methylation defines novel epigenetic subgroups of DLBCL associated with different clinical outcomes. *Blood*. 2014;123(11):1699-1708.
29. De S, Shaknovich R, Riester M, et al. Aberration in DNA methylation in B-cell lymphomas has a complex origin and increases with disease severity. *PLoS Genet*. 2013;9(1):e1003137.

30. Pan H, Jiang Y, Boi M, et al. Epigenomic evolution in diffuse large B-cell lymphomas. *Nat Commun*. 2015;6(1):6921.

31. Kalac M, Scotto L, Marchi E, et al. HDAC inhibitors and DAC are highly synergistic and associated with unique gene-expression and epigenetic profiles in models of DLBCL. *Blood*. 2011;118(20):5506-5516.

32. Kantarjian HM, Thomas XG, Dmoszynska A, et al. Multicenter, randomized, open-label, phase III trial of DAC versus patient choice, with physician advice, of either supportive care or low-dose cytarabine for the treatment of older patients with newly diagnosed acute myeloid leukemia. *J Clin Oncol*. 2012; 30(21):2670-2677.

33. Dombret H, Gardin C. An update of current treatments for adult acute myeloid leukemia. *Blood*. 2016;127(1):53-61.

34. DiNardo CD, Pratz K, Pullarkat V, et al. Venetoclax combined with DAC or azacitidine in treatment-naive, elderly patients with acute myeloid leukemia. *Blood*. 2019;133(1):7-17.